# Exclusive *p-p* Correlations from the $^{58}$Ni + $^{58}$Ni Reaction at $\approx 15$ MeV/nucleon

M. Korolija,[(1),(2)] D. Shapira,[(3)] N. Cindro,[(1)] J. Gomez del Campo,[(3)] H. J. Kim,[(3)] K. Teh,[(2)] and J. Y. Shea[(2),(4)]

[(1)]*Ruđer Bošković Institute, 41001 Zagreb, Croatia, Yugoslavia*
[(2)]*Joint Institute for Heavy Ion Research, Oak Ridge, Tennessee 37831*
[(3)]*Oak Ridge National Laboratory, Oak Ridge, Tennessee 37831*
[(4)]*Department of Physics and Astronomy, Vanderbilt University, Nashville, Tennessee 37235*

(Received 15 June 1990; revised manuscript received 29 May 1991)

Exclusive *p-p* correlations from the $^{58}$Ni + $^{58}$Ni reaction at 850 MeV incident energy have been measured. The enhancement in the *p-p* correlation function observed for small values of $\Delta p$ with a gate on $v_{\rm rel}$ is satisfactorily explained by stochastic proton emission followed by the *p-p* final-state interaction. A strong dependence of the *p-p* correlation function on the relative angle between the two-proton c.m. and the fragment velocities has been found. Also a dependence of the *p-p* correlation function on the $\Delta\mathbf{p}$ orientation with respect to the plane defined by the two-proton c.m. and the fragment velocities has been observed. This latter behavior has been attributed to angular momentum effects.

PACS numbers: 25.70.Gh, 25.70.Lm, 25.70.Np

In a number of recent heavy-ion collision studies light-particle correlations were used to obtain information on the size, lifetime, and temperature of the reaction zone [1-4]. The interpretation of the data, however, is complicated by the simultaneous action of several mechanisms that can generate correlated light particles. In particular, an enhancement of the number of correlated light particles with small relative momenta $\Delta p = \frac{1}{2}|\mathbf{p}_2 - \mathbf{p}_1|$ results from the production and subsequent decay of particle-unstable resonances [5,6]. In this picture, the information usually extracted from the correlation analysis is the initial temperature of the completely fused compound system and the multiplicity of the emitted unstable fragments.

On the other hand, for the stochastic proton emission, the interplay of the Coulomb, statistical, and nuclear effects in the final state [7,8] yields information on the source size ($r_0$) and the lifetime ($\tau$) through a source of effective size $\rho = [r_0^2 + (v_{\rm rel}\tau)^2]^{1/2}$, where $v_{\rm rel}$ is the velocity of the c.m. of the emitted pair of particles relative to the source velocity. At intermediate incident energies, light-particle emission times are typically of the order of $10^{-22}$–$10^{-21}$ s, and $\rho$ will approach $r_0$ only in the limit $v_{\rm rel} \to 0$. Obviously, the above relation can be experimentally verified only in exclusive measurements.

In this paper we study exclusive *p-p* correlations from the $^{58}$Ni + $^{58}$Ni reaction. The data were taken at the Holifield Heavy Ion Research Facility of the Oak Ridge National Laboratory using the HILI detection system [9]. In the experiment, a 1-mg/cm$^2$ $^{58}$Ni target was bombarded with an 850-MeV $^{58}$Ni beam. The charge, energy, and direction of the heavy fragment were obtained from a position-sensitive ionization chamber. Light charged particles (protons and alphas) were detected using an array of 96 $\Delta E$-$E$ phoswich scintillator detectors. The energy calibration for protons was obtained by measuring protons from the elastic scattering of the $^{58}$Ni beam from a polypropylene target at two different beam energies. The light-particle detectors had an average angular resolution of 1°. The azimuthal and polar angles of each of these detectors were calculated at the central point and then randomized over the detector area. The maximum polar detection angle was 22°.

The correlation function $R$ was calculated from the expression

$$R(\mathbf{p}_1,\mathbf{p}_2,\mathbf{p}_f)+1 = \frac{\sigma_{123}(\mathbf{p}_1,\mathbf{p}_2,\mathbf{p}_f)}{\sigma'_{123}(\mathbf{p}_{1,1},\mathbf{p}_{1,2},\mathbf{p}_{1,f};\mathbf{p}_{2,1},\mathbf{p}_{2,2},\mathbf{p}_{2,f})}\,. \quad (1)$$

Here $\sigma_{123}(\mathbf{p}_1,\mathbf{p}_2,\mathbf{p}_f)$ is the measured yield of triple-coincidence events consisting of two protons with momenta $\mathbf{p}_1$ and $\mathbf{p}_2$ and a fragment with momentum $\mathbf{p}_f$. $\sigma'_{123}(\mathbf{p}_{1,1},\mathbf{p}_{1,2},\mathbf{p}_{1,f};\mathbf{p}_{2,1},\mathbf{p}_{2,2},\mathbf{p}_{2,f})$ is the background yield of triple coincidences with components stemming from two different events (first set of indices). $\sigma'_{123}$ was constructed following a method outlined in Ref. [10]. This method selects background events of the same class as those counted in $\sigma_{123}$; thus, the background yield $\sigma'_{123}$ was constructed from events satisfying the conditions

$$|\theta_{1,f}-\theta_{2,f}| \le 1^\circ,\quad |\phi_{1,f}-\phi_{2,f}| \le 4^\circ\,,$$
$$|E_{1,f}-E_{2,f}| \le 10\ \text{MeV}\,, \quad (2)$$

where $\theta_f$ and $\phi_f$ are the fragment polar and azimuthal angles. $E_f$ is the fragment kinetic energy, while the indices 1 and 2 refer to the two different events. The described procedure was necessary since the data consisted of triple-coincidence events only, and hence it was not possible to construct one general background yield that could be applied to any set of data.

Every gate on the measured data implies the use of the same gate on the background data in order to have correct normalization properties of the ratio $R$. In that sense, the conditions (2) should ensure that the enhancement in the *p-p* correlation function stems from the effect of the *p-p* final-state interaction rather than from other possible final-state interactions or some inappropriately constructed backgrounds. As an example, let us consider the possible effect of the $p$-nucleus Coulomb final-state interaction on the $p$-$p$ correlation function. In constructing $\sigma'_{123}$ we have taken into account the heavy fragment and one proton from the same event. In this way, the influence of the $p$-nucleus Coulomb final-state interaction on the $p$-$p$ correlation function could be neglected, since the latter is defined as a ratio of the $\sigma_{123}$ and $\sigma'_{123}$ yields (which both contain the same $p$-nucleus Coulomb final-state interaction contribution). Obviously, this is a good approximation as long as the effect of the $p$-nucleus Coulomb final-state interaction is small compared with the effects of the $p$-$p$ final-state interaction. We also note that the total background yield $\sigma'_{123}$ was obtained by treating each measured event on equal footing, i.e., by putting all measured events in a "big box" and taking into account all possible combinations of the measured events from the big box.

Figures 1(a) and 1(b) show the $p$-$p$ correlation functions for heavy-ion fragments with charges in the range $21 \le Z \le 26$. The data are with (open symbols) and without (solid symbols) a gate on the relative velocity $v_{\rm rel} = |\mathbf{v}_{pp} - \mathbf{v}_f|$. To determine the fragment velocity $\mathbf{v}_f$ from $\mathbf{p}_f$ for each fragment of a given charge $Z$, we have taken the most probable mass obtained from a distribution calculated with a statistical evaporation code LILITA [11]; $\mathbf{v}_{pp} = (1/2m_p)(\mathbf{p}_1 + \mathbf{p}_2)$ is the $p$-$p$ center-of-mass velocity in the laboratory frame ($m_p$ is the proton mass). Figure 1(a) shows the $p$-$p$ correlation function with all the three particles detected above the beam axis (geometry I, see top of the figure). Similarly, Fig. 1(b) shows the same for a configuration where the two light particles are detected above and the heavy fragment below the beam axis (geometry II). Notice that only geometry I can detect the two light particles in a small angular cone around $\mathbf{v}_f$; Fig. 1(a) shows that this geometry yields the strongest $p$-$p$ correlations.

The distributions of $v_{\rm rel}$ measured in the two geometries are shown in Figs. 2(a) and 2(b). The effect of selecting events with small $v_{\rm rel}$ (shaded areas in Fig. 2) is illustrated in Fig. 3. By comparing proton (a) and heavy-fragment (b) spectra from Fig. 3, it comes out straightforwardly that low- and high-energy protons are accompanied by quasielastic and deep-inelastic heavy

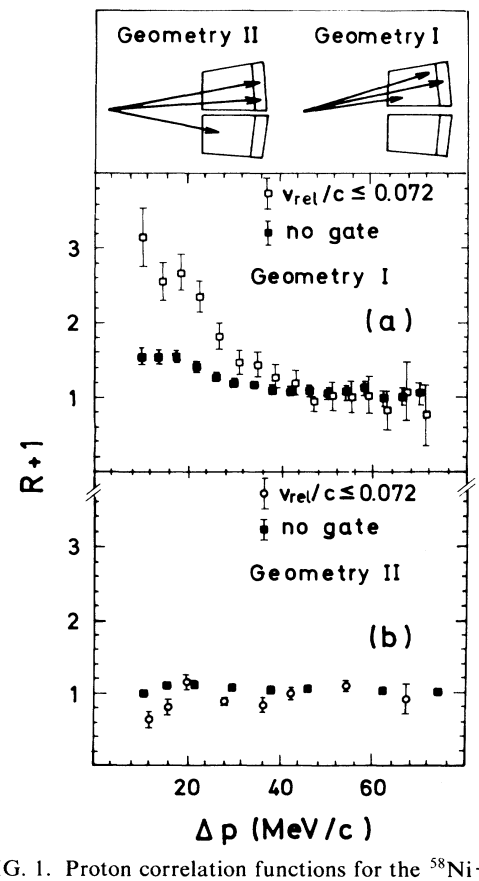


FIG. 1. Proton correlation functions for the $^{58}Ni + ^{58}Ni$ reaction at 850 MeV incident energy for two different experimental arrangements shown on top. The proton correlation functions with no gate on the data (solid symbols) and with a gate on $v_{\rm rel}$ (open symbols) are shown for (a) geometry I and (b) geometry II. Errors reflect statistical uncertainties only.

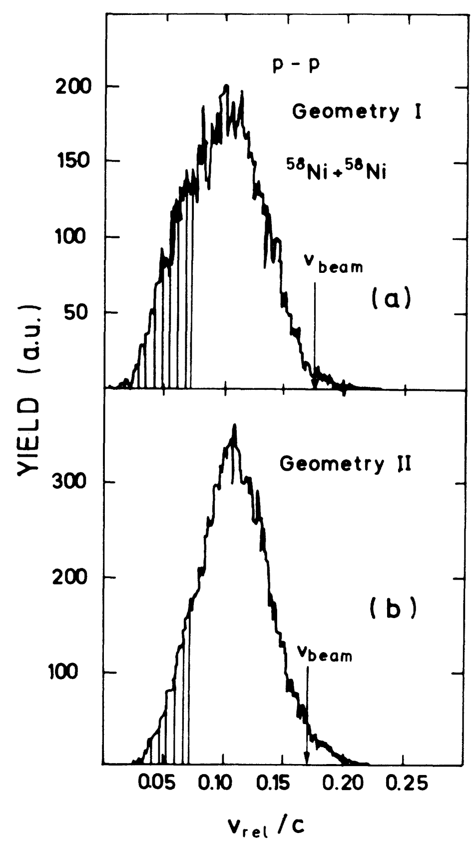


FIG. 2. Distribution of $v_{\rm rel}$ for (a) geometry I and (b) geometry II. The arrows show the beam velocity ($v_{\rm beam}$).

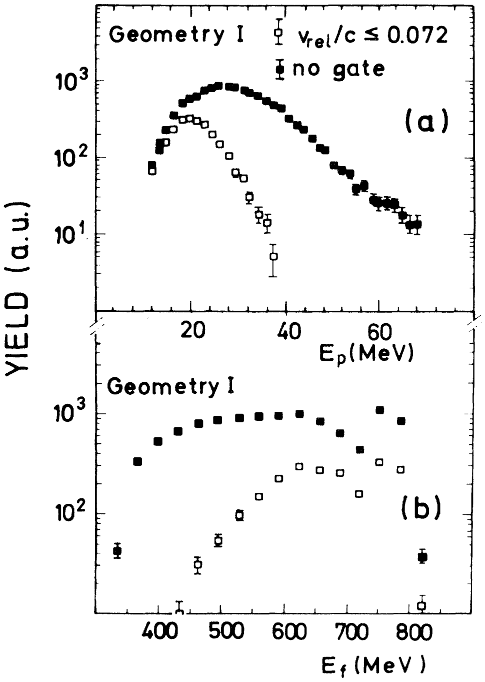


FIG. 3. (a) Proton and (b) fragment kinetic-energy spectra for geometry I. Symbols are as in Fig. 1(a).

fragments, respectively. Furthermore, under the assumption of binary reactions in the incident channel, the "gate-on" and "no-gate" data from Fig. 3(b) overlap in a broad range of fragment excitation energies around $E^* \sim 100$ MeV ($E_f \sim 650$ MeV). Thus, in what follows, we shall relate the extracted source size and the lifetime to fragments in this excitation energy range. Furthermore, the source is assumed to be spherical with a constant mean size during the reaction.

The thermodynamical statistical model [12] predicts the production, followed by subsequent decay, of unstable fragments from the compound system at sufficiently high excitation energy or emission temperature. The contribution of this process in the case of geometry I, where the strongest *p-p* correlations were observed, was estimated with the Hauser-Feshbach program BUSCO [13]. In calculating the ratio of $2p$ vs $^2$He yield we included angular ($\pm 3°$) and momentum ($\Delta p = 20 \pm 3$ MeV/$c$) constraints and took into account the actual solid angle covered by the HILI detection system. Then, by taking for the $^{58}$Ni excitation energy $E^* = 150$ MeV and for the angular momentum $J_{max} = 50\hbar$ we obtained a factor of $\sim 10^2$ in favor of $2p$ vs $^2$He emission.

The source size $r_0$ and lifetime $\tau$ were determined from the comparison of the extracted *p-p* correlation functions with the calculations obtained using the *p-p* final-state interaction model from Ref. [7]. Figure 4 shows the extracted *p-p* correlation functions for $\Delta \mathbf{p}$ projected in the $\mathbf{v}_{rel}$ direction ($\Delta p_{\parallel}$) and the corresponding fits obtained by taking $\Delta p_{\perp} = 0$. We analyzed *p-p* correlation functions projected in the $\mathbf{v}_{rel}$ direction since in this direction the

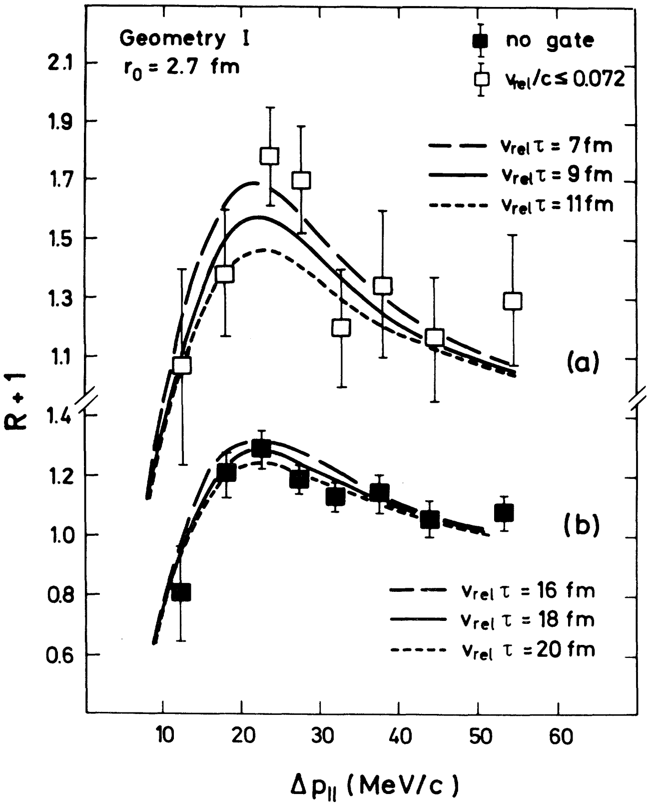


FIG. 4. Proton correlation functions vs the value of $\Delta \mathbf{p}$ projected on the $\mathbf{v}_{rel}$ axis ($\Delta p_{\parallel}$) for $^{58}$Ni+$^{58}$Ni at geometry I. Lines show calculations of the *p-p* correlation function obtained using the model of Ref. [7], for $\Delta \mathbf{p} \parallel \mathbf{v}_{rel}$. Symbols are as in Fig. 1(a).

*p-p* correlation function is mostly sensitive to lifetime effects [14]. The finite resolution of the hodoscope elements has been taken into account in the calculations. Open squares correspond to the *p-p* correlation functions obtained with a gate on $v_{rel}$; while solid squares correspond to a measurement without gate. The lines refer to fits obtained following Ref. [7] by taking $r_0 = 2.7$ fm and varying $v_{rel}\tau$ in the range $9 \pm 2$ [Fig. 4(a)] and $18 \pm 2$ fm [Fig. 4(b)].

The best-fit values of the source size ($r_0$) and the lifetime ($\tau$) were determined using the following procedure. First, the value of the source size of 2.7 fm and parameter $v_{rel}\tau = 9 \pm 2$ fm were obtained from the fit to the *p-p* correlation function measured for the data gated with $v_{rel}$ (open squares). Then, assuming a constant source size, the value of the parameter $v_{rel}\tau = 18 \pm 2$ fm was obtained from the fit to the ungated *p-p* correlation function. To obtain the average lifetime $\tau$ we used for $v_{rel}$ the average values from Fig. 2(a). The gate-on condition yields $\langle v_{rel} \rangle = 0.06c$, while the no-gate condition yields $\langle v_{rel} \rangle = 0.10c$. Introducing these values into the fit values for $v_{rel}\tau$ (Fig. 4), we obtain source-lifetime values $(3.9 \leq \tau \leq 6.1) \times 10^{-22}$ s and $(5.3 \leq \tau \leq 6.6) \times 10^{-22}$ s for the gate-on and no-gate conditions, respectively.

In the model of $p$-$p$ final-state interactions of Ref. [7] the influence of the angular momentum involved in the reaction on $p$-$p$ correlations is not included. On the other hand, the influence of angular momentum effects on two-neutron correlations was discussed in Ref. [15], where it was shown that the $n$-$n$ correlation function does depend on angular momentum effects. The neutrons were assumed to originate from the rapidly spinning compound nucleus with no $n$-$n$ final-state interaction. Therefore, a similar dependence of the $p$-$p$ correlation function on the angular momentum could be expected too. If such dependence is experimentally observed, it will affect the extracted source sizes. This can be understood from the following simple consideration. When the source possesses high angular momentum, a given direction for particle emission is preferred. This results in an effective lowering of $\Delta p$, because components of $\Delta p$ in the direction perpendicular to the preferred one will be very small. Since the correlation function depends on the product $\Delta p \Delta r$, angular momentum effects would directly influence the extracted source sizes. In this respect, Figs. 5(a) and 5(b) show the dependence on the total $p$-$p$ coincidence yield on the direction of $\mathbf{\Delta p}$ relative to the plane spanned by the vectors $\mathbf{v}_{pp}$ and $\mathbf{v}_f$ (see inset). The angle $\theta_n$ between the normal $\mathbf{n}$ on this plane and $\mathbf{\Delta p}$ was computed for each event. While the data averaged over the whole $v_{\rm rel}$ distribution [no gate, Fig. 5(a)] show no dependence on the particular slice of $\theta_n$, the data with a gate on $v_{\rm rel}$ [Fig. 5(b)] show a different pattern. The maximum in the $p$-$p$ coincidence yield corresponds to such events where all three vectors $\mathbf{v}_f$, $\mathbf{v}_{pp}$, and $\mathbf{\Delta p}$ are essentially coplanar ($60° \le \theta_n \le 90°$). The strong dependence of the $p$-$p$ correlation function on the orientation of $\mathbf{\Delta p}$, observed in this work, suggests the necessity of including angular momentum effects into the $p$-$p$ final-state interaction theory.

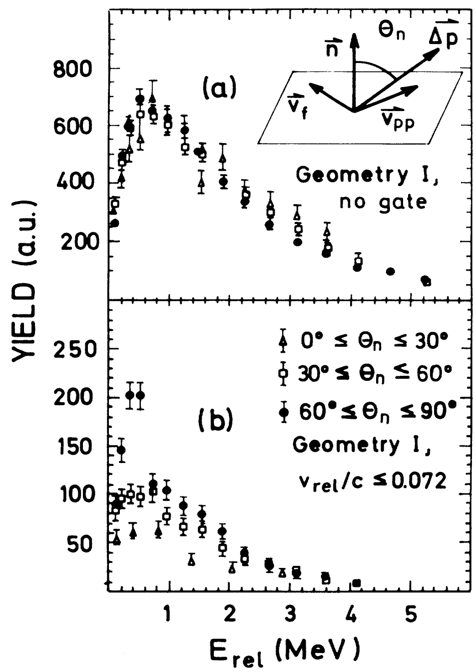


FIG. 5. Total $p$-$p$ coincidence yield for $^{58}$Ni+$^{58}$Ni data with (a) no gate and (b) with a gate on $v_{\rm rel}$ for geometry I. Symbols in both parts refer to total triple-coincidence yields for the $\theta_n$ slices shown in (b).

In summary, the $p$-$p$ correlation function has been measured for the $^{58}$Ni+$^{58}$Ni reaction at $E_{\rm inc}$=850 MeV. The observed enhancement of the $p$-$p$ correlation function for small $\Delta p$ values is interpreted as a result of the interaction of the emitted protons in the final state. The interpretation of this enhancement as a result of the production and subsequent decay of the unstable resonance $^2$He is ruled out on the grounds that the expected production of $^2$He is small in the analyzed range of the fragment excitation energy. On the other hand, the $p$-$p$ correlation function has been found to decrease very rapidly with the increase of the relative angle between the fragment and the two-proton c.m. velocities. The maximum in the $p$-$p$ correlation function observed when the velocity vectors of all three particles are coplanar is interpreted as a result of angular momentum effects. This calls for the inclusion of angular momentum effects into the $p$-$p$ final-state interaction theory.

This paper is part of a study under the U.S.–Yugoslav Collaboration Project No. JF 939 DOE/IRB. ORNL is operated by Martin Marietta Energy Systems, Inc., under Contract No. DE-ACO5-840R21400 with the U.S. Department of Energy.


[1] D. Fox *et al.*, Phys. Rev. C **38**, 146 (1988), and references therein.

[2] T. S. Awes *et al.*, Phys. Rev. Lett. **61**, 2665 (1988).

[3] D. A. Cebra *et al.*, Phys. Lett. B **227**, 336 (1989).

[4] P. A. de Young *et al.*, Phys. Rev. C **39**, 128 (1989).

[5] M. A. Bernstein *et al.*, Phys. Rev. Lett. **54**, 402 (1985).

[6] P. D. Bond and R. J. de Meijer, Phys. Rev. Lett. **52**, 2301 (1984); W. G. Lynch *et al.*, Phys. Rev. Lett. **52**, 2302 (1984).

[7] S. E. Koonin, Phys. Lett. **70B**, 43 (1977).

[8] R. Lednicky and V. L. Lyuboshits, Yad. Fiz. **35**, 1316 (1982) [Sov. J. Nucl. Phys. **35**, 770 (1982)].

[9] D. Shapira *et al.*, Nucl. Instrum. Methods Phys. Res., Sect. A **301**, 76 (1991).

[10] W. A. Zajc *et al.*, Phys. Rev. C **29**, 2173 (1984).

[11] J. Gomez del Campo and R. Stokstad, ORNL Report No. TM7295, 1981 (unpublished).

[12] W. A. Friedman and W. G. Lynch, Phys. Rev. C **28**, 16 (1983); M. A. Bernstein, W. A. Friedman, and W. G. Lynch, Phys. Rev. C **29**, 132 (1984).

[13] J. Gomez del Campo *et al.*, Phys. Rev. Lett. **61**, 290 (1988).

[14] S. Pratt and M. B. Tsang, Phys. Rev. C **36**, 2390 (1987).

[15] S. E. Koonin, W. A. Bauer, and A. Schäfer, Phys. Rev. Lett. **62**, 1247 (1989).